ENHANCING THE PERFORMANCE OF TITANIUM SURFACE VIA ELABORATION OF A NANOSTRUCTURE AND A BIOACTIVE COATING

Mihaela GRECU[1], Mariana PRODANA[2], Anişoara CÎMPEAN[3], Daniela IONIȚĂ[4]

Lucrarea este focalizată pe elaborarea unei noi metode de creştere a performanţelor unei suprafeţe de titan ca biomaterial, prin efecte sinergice, prin realizarea de nanostructuri şi acoperiri bioactive. Nanoarhitectura constă din nanotuburi de TiO_2 iar hidroxiapatita serveşte ca înveliş ceramic bioactiv. S-au efectuat analize de suprafață prin microscopie SEM, AFM precum si măsurări de unghi de contact. Comportamentul electrochimic al arhitecturii hibride (nanotuburi+ înveliş ceramic) este discutat în funcție de parametrii curbelor de polarizare şi de concentrația de ioni eliberați şi este corelat cu biocompatibilitatea. Se realizează astfel o performanță superioară a noii nanoarhitecturi.

The paper focuses on new method of enhancing the performance of titanium biomaterial directly onto material surfaces, via synergistic effects such as the elaboration of a nanostructure and bioactive coating. The nanoarchitecture consists in TiO_2 nanotubes, while hydroxyapatite serves as bioactive ceramic coating. Surface analysis such as SEM, AFM microscopy and contact angle measurements were performed. The electrochemical behaviour of the hybrid architecture (nanotubes + ceramic coating) is discussed in terms of polarization curves and concentration of released ions and it is correlated with biocompatibility data. Thus, a better performance of the new nanoarchitecture is obtained.

Keywords: Titanium, corrosion, TiO_2 nanotubes, hydroxyapatite coating, nanostructure

1. Introduction

Many efforts have been made to improve the performance of implant materials such as titanium and its alloys [1-3]. Potential applications of titanium

[1] PhD student., Facultyof Chemistry and Materials Science, University POLITEHNICA of Bucharest, Romania, e-mail: ela.grecu@gmail.com
[2] Eng., Facultyof Chemistry and Materials Science, University POLITEHNICA of Bucharest, Romania, e-mail:
[3] Prof., Facultyof Chemistry and Materials Science, University POLITEHNICA of Bucharest, Romania, e-mail:
[4] Prof., Facultyof Chemistry and Materials Science, University POLITEHNICA of Bucharest, Romania, e-mail:

based biomaterials are for instance keywords for numerous papers [4, 5]. This trend in the current research [6] is explained by the very good corrosion resistance and good mechanical properties of titanium, due to its native protective oxide layer (TiO_2) spontaneously formed on its surface when exposed to air or other oxygen containing media. This native oxide passive layer is typically 2 to 5 nm thick and is responsible for chemical stability in various environments including bioliquids [7].

A number of procedures were proposed in order to enhance TiO_2 electrochemical stability [8, 9] since corrosion in various bioliquids could be aggressive. According to the Tomashov approach [10], greater effectiveness of corrosion control may be achieved by using more than one method of protection. Our paper combines the nanotube architecture with a biomimetic phosphate coating with the goal of obtaining synergistic effects in decreasing the corrosion rate of Ti in bioliquids. The fundamental classification of corrosion control [11] established various methods for reaching efficiency, including an increase of thermodynamic stability of the coating system; this idea is applied here to build a nanoarchitecture, taking into account that the behaviour of materials at nanolevel leads in many cases to remarkable improvement of their properties. By monitoring the TiO_2 nanoarchitecture, new applications and enhancements of well known TiO_2 properties can be found [12]. In this approach, various techniques have been tested in order to get better micro and nanostructure [13], and TiO_2 nanotubes structure was found to be a promising alternative [14]. For potential applications in implant materials, induced bioactivity has already been proposed, and phosphate such as hydroxyapatite [15] has been used as bioactive coating [16, 17] due to the presence of Ca and P elements in the inorganic part of the bone. Such coating exhibits a better electrochemical behaviour [18]; furthermore, having the same components in elemental composition, the host response is friendlier. On the other hand, bone minerals being at nanoscale, the research has been directed on improving the properties of nanosize phosphates [19]. In order to obtain a better fitting of the implant into the body (*i.e.* a better biointerphase), the contribution of the present study is to combine the benefit of a ceramic coating with the capacity of a nanostructure (such as nanotube) to enhance bioperformance. Anodizing in mixtures with fluoride was chosen as elaboration procedure of the nanotubes. Regarding elaboration of controllable properties of oxide self organized layers on Ti surface, various nano-modification techniques [20, 21] have permitted in the last decade the creation of structures possessing nanometer surface features able to improve the contact-bonding ability between the implant and bone due to the increased surface area of the implant nanoarchitecture [22]. By monitoring anodizing parameters (such as voltage, pH, electrolyte compositions and time of electrolysis), a large variety of structures [11, 20] has been identified. In this paper nanotubes with diameter of 60nm were chosen. The coating metallic implants

with biologically active materials, *e.g.* hydroxyapatite (HA) or other phosphates with mimetic features of natural bone may reduce metallic ion release by acting as a barrier and accelerate the bone formation on the initial stage of osseointegration [23-27].

In this study the biocompatibility evaluation was accomplished for cell cultures on native TiO_2 and on TiO_2 obtained after anodizing in conditions with and without of nanotubes formation. It is known [28] that the fibroblasts prefer smooth surface, whereas osteoblasts prefer rougher surfaces, but it is to point out that other surface properties as hydrophilic/hydrophobic balance may affect the bioperformance results, as well [28].

2. Experimental Part

2.1. Samples preparation

Titanium samples used for the present study were 99.6% purity, provided by the Institute for Non-Ferrous and Rare Metals, Bucharest. Rectangular specimens 10×10×1 mm in size were cut from a titanium plate. As a pretreatment procedure, the specimens were mechanically polished with SiC grinding paper (ultimate grid size 1500), cleaned by a mixed HF/HNO_3 solution, rinsed with ethanol and deionised water, and subsequently air-dried. The group numbers of the specimens were assigned to the different processing conditions as follows: S1 – pretreated Ti, as a control; S2 - Ti sample which was pretreated and anodized in 1 M H_3PO_4; S3 - Ti sample which was pretreated and anodized in HF 0.5% + 5g/L Na_2HPO_4 (in order to obtain nanotubes).

The anodizing procedure implied a two-electrode cell configuration with a working electrode and a carbon counter electrode. The anodizing conditions regarding electrolyte solutions, time, and voltage are given in Table 1. The experiments were conducted at room temperature.

Table1

The anodizing conditions

Samples and electrolytes	Time (min)	Voltage (V)
S1	-	-
S2 (1 M H_3PO_4)	60	60
S3 (HF 0.5%+5g/L Na_2HPO_4)	120	20

For electrochemical behaviour Hank solution was chosen as testing solution [29]; its composition was: NaCl 0.1369 mol/L; $CaCl_2.2H_2O$ 0.0013 mol/L; KCl 0.0054 mol/L; $Na_2HPO_4 \cdot 2H_2O$ 0.0003 mol/L, KH_2PO_4 0.0004 mol/L,

$MgSO_4 \cdot 7H_2O$ 0.0008 mol/L, glucose 0.005 mol/L. All tests were performed at 37^0C.

For the sample with nanostructure according to a chemical immersion procedure for different times the phosphate layer was obtained. The composition of the immersion electrolyte, the simulating body fluid (SBF), was: NaCl 0.11 mol/L; $NaHCO_3$ 0.02 mol/L; KCl 0.005 mol/L; $Na_2HPO_4 \cdot 2H_2O$ 0.1 mol/L, $MgCl_2 \cdot 6H_2O$ 0.002 mol/L; $CaCl_2$ 0.003 mol/L, $NaSO_4$ 0.0005 mol/L.

The solution was adjusted to a pH value of 7.4 with tris-hydroxymethylaminomethane [$(CH_2OH)_3CNH_2$] and hydrochloric acid and the temperature was kept at 37^0C.

2.2. Samples characterization

Surface morphology and chemical analyses were performed using scanning electronic microscopy (SEM) type Philips provided with a equipment for energy-dispersive X-ray spectroscopy (EDS). This system enabled us to evaluate both the surface changes in respect with pore or nanotube diameter and elemental composition (formed after the treatments). The roughness of the surface of the prepared specimens was quantified using atomic force microscopy (AFM) equipment type A.P.E. Research. The surface analysis was sustained by contact angle determination, to evaluate the hydrophilic/hydrophobic balance. In order to evaluate the wettability of the modified surface as a result of changing structure and composition the contact angle measurements were carried out with 100 Optical Contact Angle Meter - CAM 100. The liquid used for contact angle measurement was distilled water. The structure of the coatings after immersion in SBF was identified with FTIR spectroscopy using an equipment type ATR Perkin-Elmer.

Corrosion tests. The corrosion measurements were conducted with *Voltalab PG 301* potentiostatic assembly with three electrodes in a single-compartment cell, using platinum as a counter-electrode and saturated calomel (SCE) as reference electrode. Cyclic polarization tests were recorded taking into account the ASTM F 2129-01 [30]. In these tests the open circuit potential was monitored for 1 hour prior to begin the cyclic scan. Potentiodynamic polarization curves were carried out with a scan rate of 1 mV/s in the potential range from −800 mV to 2500 mV vs SCE. The titanium samples S1, S2 and S3 uncovered and covered with Ca-P were electrochemically polarized in Hank solution.

Cell culture. Human gingival fibroblasts (HGF-1, CRL-2014, American Type Culture Collection) were seeded at an initial density of $1x10^4$ cells cm^{-2} in a Dulbecco's Modified Eagle Medium (DMEM) containing 10% fetal bovine serum (FBS) and 100 U/mL penicillin and 100 μg/mL streptomycin, in an humidified atmosphere with 5% CO_2.

The cells were plated at the same density on S1, S2 and S3 samples and were cultivated at least 72h before viability evaluation. To estimate the density of viable cells by measuring mitochondrial dehydrogenase activity a MTT (3-(4, 5-dimethylthiazolyl-2)-2, 5-diphenyltetrazolium bromide) assay was employed. MTT assay measures the cell activity, proliferation rate and cell viability. The yellow tetrazolium MTT is reduced by metabolically active cells, in part by the action of dehydrogenases, to the corresponding blue formazan. The formazan crystals were solubilized with isopropanol and absorbance of the supernatant was measured at 550 nm. The absorbance measured at a wavelength 550 nm is proportional with number of viable cells. MTT assay was repeated three time for each case.

ICP-MS determination. For Ca^{2+} and Ti ions release determination an ELAN DRC-e inductively plasma mass spectrometer was used (ICP-MS). All samples (typically: 0.1–1.2 mg) were digested in 100 mL concentrated nitric acid (ULTRAPURE, Fa. Merck). Acid digestion was performed in a well determined volume of HNO_3 65%; after digestion, the samples were diluted 100 times and liquid fractions were analyzed.

Statistical analysis. Each experiment was repeated and results are expressed as an average of triplicate determinations. The terms Single Factor Analysis of Variance, Single Factor ANOVA, One Way Analysis of Variance, and One Way ANOVA are used interchangeably to describe the situation where a continuous response is being described in terms of a single factor exhibiting two or more levels (categories).

3. Results and Discussion

3.1. Surface analysis

Fig. 1a shows the morphology of pure titanium (S1) and Figs. 1b and 1c illustrate the anodized titanium surfaces S2 and S3 respectively. The control surface (S1) exhibited shallow parallel grooves oriented along the polishing direction. This is the well known structure of native passive layer, a mixture of titanium oxides with predominant TiO_2, as was presented in a previous work [13]. The S2 surfaces displayed island-shape films with irregular micro-pores generated by sparking during anodic oxidation.

SEM image for S3 sample (Fig.1c) shows the appearance of TiO_2 nanotubes with a diameter of 60 nm. The EDS chemical analysis of TiO_2 nanotube exhibits that the concentration of Ti atoms is around 33% and that of oxygen atoms is about 67% for this nanoporous layer. This result implies that the nanotube array is composed of TiO_2.

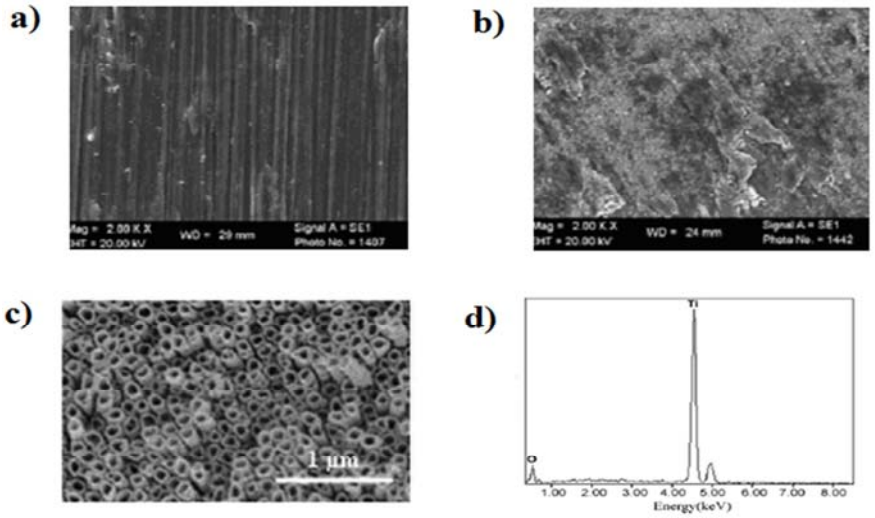

Fig. 1. SEM images of the samples: a) S1, b) S2, c) S3; Fig. 1-d shows the EDS spectrum of nanotube

The Roughness Average (R_a) and Root Mean Square (RMS) for S3 samples are 47 nm and 58 nm compared with 11 and 27 nm, that are respectively values for S1 samples. For the sample S2 the roughness characteristics are 32 and 44 nm, respectively (Table 2). The AFM images used for such roughness evaluation are presented in Figs. 2 a-c.

Table2

The values of contact angle and roughness for all samples before/after 3 days immersion in SBF

Sample	R_a (µm)		RMS (µm)		Contact angle (deg)	
	before immersion	after immersion	before immersion	after immersion	before immersion	after immersion
S1	0.11±0.1	0.27±0.21	0.15±0.17	0.33±0.18	77	49
S2	0.32±0.15	0.44±0.25	0.46±0.15	0.54±0.15	52	40
S3	0.47±0.12	0.58±0.20	0.82±0.1	0.72±0.15	38	25

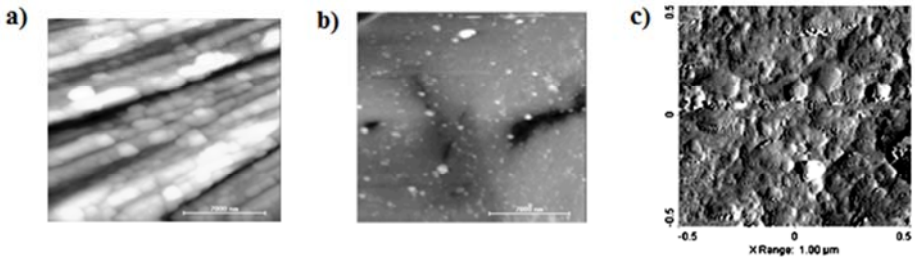

Fig. 2. AFM images of samples a) S1, b) S2, c) S3

Regarding contact angle values, it is to point out that for all studied structures the experimental data indicated a hydrophilic behaviour.

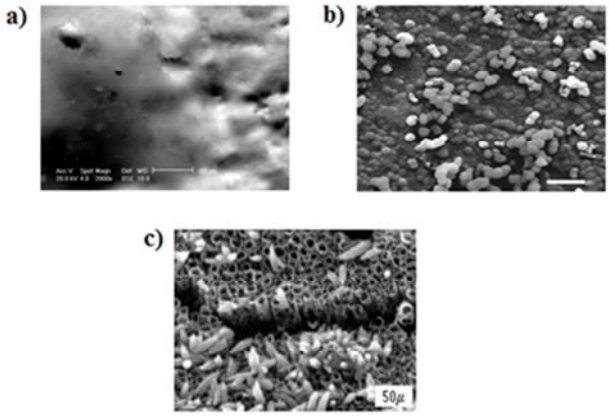

Fig. 3. Phosphate appearance on film deposited in SBF a) after72 h on S1, b) after 66 h on S2; c) after 48h on S3.

After depositing the hydroxyapatite (HA), the corresponding surfaces had remarkably reduced contact angles. Interestingly, the decrease of contact angles was related to the contact angles of the substrate surfaces, *i.e.* the surfaces before deposition of nano HA. The decrease of contact angles by HA deposition is ascribed to high surface energy of nano HA particles. Ca^{2+} and PO_4^{3-} ions as hydrophilic solutes in the surface oxides, promote surface hydration resulting in a decrease of contact angles.

Obviously, the nanotubes have contributed to the increase of surface roughness and surface area. Also, a rougher surface provided by TiO_2 promoted mechanical interlocking between coating and TiO_2. The nanotube structure of TiO_2 should serve as anchorage of phosphate coating as can be seen in Fig. 3c.

It should be pointed out that no phosphate was found on the native passive TiO_2 immersed in SBF for the same period of time; this is an evidence in support

of the ability of nanostructure to promote surface bioactivation inducing phosphate formation. On native passive layer, nucleation of phosphate appears only after 3days in SBF according to Fig. 3a, and the film is not a uniform one. The elemental EDS result indicates a Ca/P ratio of 1.28, close to octocalcium phosphate formula OCP-$Ca_8(HPO_4)_2(PO_4)_4$ $5H_2O$ which is 1.33 [31].

As can be seen from the SEM image (Fig. 3c), the surface was not entirely coated after 2 days of immersion in SBF, providing a likely explanation for the non-significant change of hydrophilicity (34^0 angle for S3 sample). Despite the nonuniformity of the coating obtained in SBF, the presence of phosphate becomes clear after a few days, as the structural analysis of coatings presented in Figs. 4a and 4b shows.

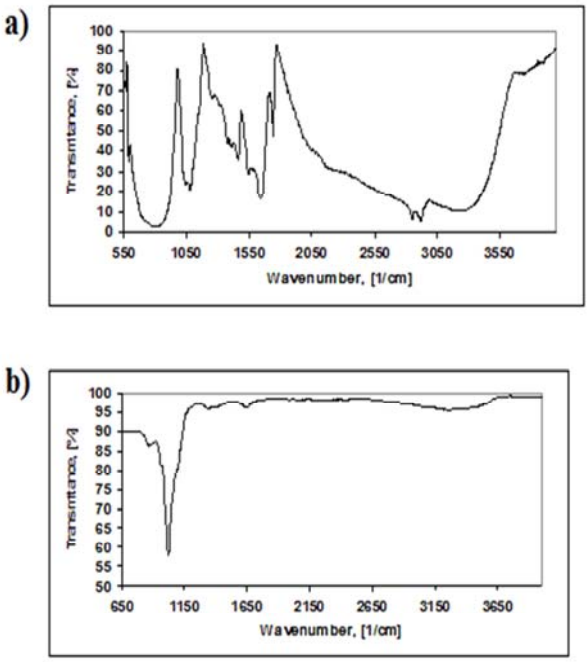

Fig. 4. FT-IR spectra of phosphate deposition a) on TiO_2 nanotubes b) on native passive layer

These figures are devoted to FT-IR analysis, in the transmittance mode for the coated nanotubes TiO_2 (S3) in SBF after 2 days immersion and for coated native passive layer (S1) after 3 days immersion. A calcium-phosphate deposit was detected on the surface electrode, based on the presence of phosphate group at 565cm^{-1} and 616 cm^{-1} representing ν_4 O-P-O bending vibration and hydroxyl group at around 3240 cm^{-1} and 1640 cm^{-1}. According to literature data [32] the

616 cm^{-1} band is a suggestion for appearance of a crystalline octocalcium phosphate, a precursor of hydroxyapatite.

The coating was more uniform and more stable after longer periods of immersion according to electrochemical results and ions release measurements.

The covering with hydroxyapatite was completed at different times: for S1 in 21 days, for S2 in 7 days and for S3 in 3 days.

The SEM images and EDS spectra for the samples are presented in Figs. 5a, 5b and 5c. The Ca/P ratio in all cases is fairly close to such ratio in bones.

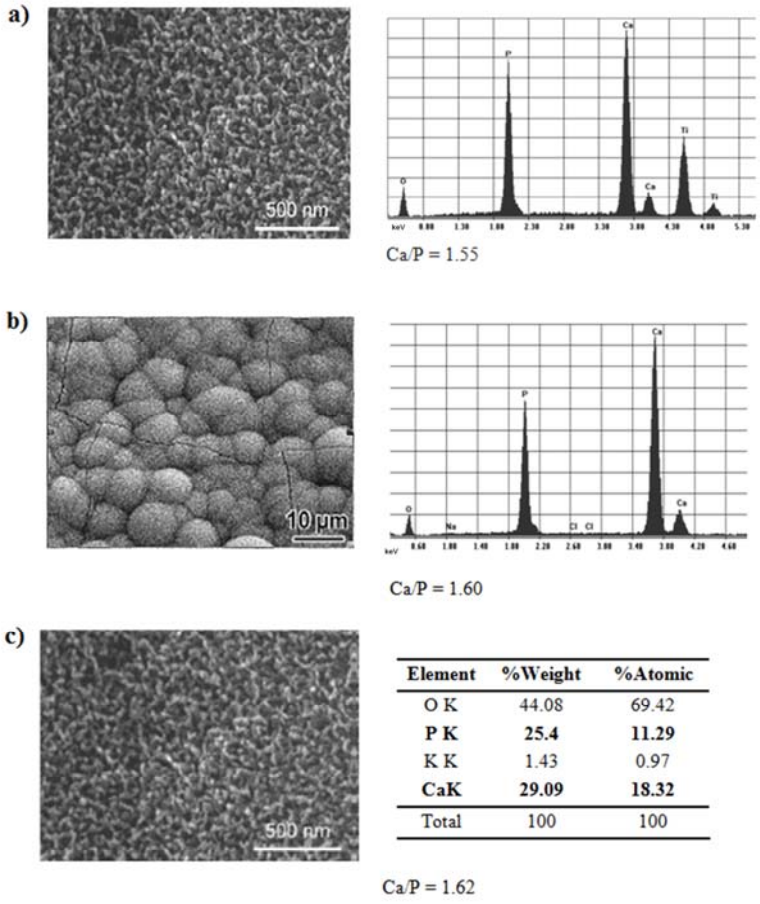

Element	%Weight	%Atomic
O K	44.08	69.42
P K	**25.4**	**11.29**
K K	1.43	0.97
CaK	**29.09**	**18.32**
Total	100	100

Ca/P = 1.62

Fig. 5. SEM image and EDS spectra for samples a) S1after 21 days of immersion in SBF, b)S2 after 7 day immersion in SBF c) SEM image and table with elemental analysis of S3 after 3 days of immersion in SBF.

The closer ratio is in the case of S3 and such behaviour sustains a better osteointegrations as well.

3.2. The results of corrosion tests

The titanium behaviour is due to a passive TiO_2 oxide, which suffers a hydrolysis process by immersion in bioliquids, independent on its micro or nanostructure and an equilibrium surface-solution is established. In the case of nanotubes, due to the model of their formation [33-35], more complex various ions are involved; but for both native passive structure and nanotubes, a dissolution phenomenon may lead to species such as $Ti(OH)_2$ or hydroxocomplex like $TiO(OH)_2$. The tendency towards steady state is more evident for TiO_2 nanotubes after a shorter period of time as can be observed in open potential circuit determinations [6]. The dissolution and repassivation of Ti are expressions of the electrochemical passivity in both cases. As a measure of coating phosphate stability, the polarization curves recorded using Hank solution permitted evaluation of corrosion rate. The potentiodynamic polarization curves for S1, S2 and S3 are presented in Figs. 6a and 6b before and after immersion in SBF. The shape of polarization curves indicated passive behaviour. The current density achieved a constant value (i_{pass}) on anodic polarization without exhibiting any active – passive transition.

Electrochemical parameters from Tafel plots before and after immersion in SBF for various periods of time are listed in Table 3.

Table 3

Electrochemical parameters from Tafel plots

Samples	E_{corr} (mV) vs. SCE	I_{corr} ($\mu A/cm^2$)	v_{corr} (mm/y) by potentiodynamic measurements	v_{corr} (mm/y) by ICP-MS measurements
S1	-205	9.6	6.82×10^{-2}	6.128×10^{-2}
S1 after 21 days immersion on SBF	-117.8	0.7	6.8×10^{-4}	6.4×10^{-4}
S2	-241	5.6	4×10^{-2}	3.7×10^{-2}
S2 after 21 days immersion in SBF	-127	2.1	1.5×10^{-2}	
S3	62.4	1.97	1.09×10^{-2}	0.89×10^{-3}
S3 after 21 days immersion in SBF	470	0.014	1.67×10^{-4}	1.65×10^{-4}

It is clear from the calculated values that coated TiO_2 nanotubes increase the surface stability by reducing the corrosion current densities and corrosion rate, especially after longer period of immersion time in SBF.

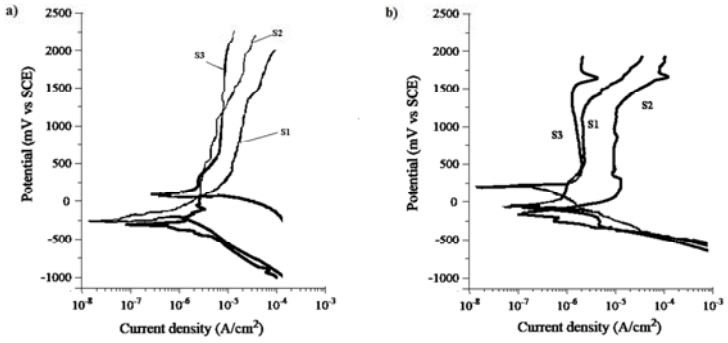

Fig. 6: (a) Potentiodynamic polarization curves for S1, S2, and S3 samples tested in Hank solution
(b) Potentiodynamic polarization curves for S1, S2, and S3 samples tested in Hank solution after 21 days immersion in SBF

The immersion in SBF is a way of obtaining biomimetic coating, and the infrared spectra indicate appearance of phosphate acting as a barrier controlling corrosion resistance in bioliquid. This ability to form phosphate represents at the same time an aspect of bioperformance.

Potentiodynamic curves indicated that the corrosion current densities obtained by Tafel lines extrapolation decrease in the following order: $i_{corr\ S1} > i_{corr\ S2} > i_{corr\ S3}$. According to Table 3, all corrosion rates for various Ti/TiO_2 electrodes in Hank solution correspond to various class of stability [36] from stable to perfect stable. Comparing behaviour before immersion in SBF, the TiO_2 nanoarchitecture of sample S3 structure has the smallest corrosion rate, confirming the literature data [20, 37] regarding enhancing corrosion resistance in bioliquid *via* elaboration of TiO_2 nanotubes. The smallest corrosion rate from Table 3 which sustained the best stability is for nanotubes fabricated in the mixture HF 0.5%+5g/L Na_2HPO_4 and coated with phosphate. The corrosion rate for this sample, S3 immersed in SBF is around 425 times less than corrosion rate in the case of Ti covered with native passive TiO_2 film (S1). Such behaviour sustains the synergistic effect of the hybrid structure (nanotubes + ceramic coating) on the Ti implant material performance, taking into account that, after immersion in SBF, the native passive TiO_2 is only 100 times more stable. Regarding the corrosion potential values, a shift from electronegative value to more noble values is observed according to the following series: $E_{corr\ S3} < E_{corr\ S1} < E_{corr\ S2}$.

The hybrid sample with nanotubes and hydroxyapatite remains the most stable one.

The current density of samples S1, S2, S3 after 21 days immersion in SBF shows a passive region with current densities between 10^{-5} - 10^{-7}A/cm^2, whereas that of the Ti samples before immersion is about of 10^{-4} – 10^{-6} A/cm^2. From Fig. 6b the corrosion current density of samples after immersion at passive region is smaller than that of the before immersion, indicating the good Ca-P film growth with dense layer formation.

3.3. ICP-MS determinations

Fig. 7 shows the calcium concentration changes in the Hank solution during 30 days immersion for sample S3 and sample S1. In the cases of sample S3 the coating first dissolved after 5 days immersion. As can be observed from Fig. 7, the calcium concentration changes with time can be divided into three stages. In the first stage - dissolution process at coating - the calcium release rapidly increased with time. After this stage, the increase in calcium was continued with a lower rate compared to the previous stage. A reprecipitation process to rebuild the initial HA deposit from Day 5 up to Days 12-14 occurred at this stage. The third stage is an additional precipitation process to thickening the HA deposit after Day 14. The evolution of Ca ion release indicates that three mathematical functions can be used to fit the dissolution curves, as given in Table 4.

Table 4

Analytical functions used to fit the dissolution process

Stage	Function	R^2
I-dissolution	$y = 0.047 \ln x + 0.0984$	0.9868
II - reprecipitation	$y = -0.006x^2 + 0.0131x + 0.123$	0.9989
III-additional precipitation	$y = 7 \cdot 10^{-5} x^2 - 0.039x + 0.225$	0.9924

The experimental point which separates the analytical function should be chosen for each curve so that suggested functions have the best approximation (R^2)**.**

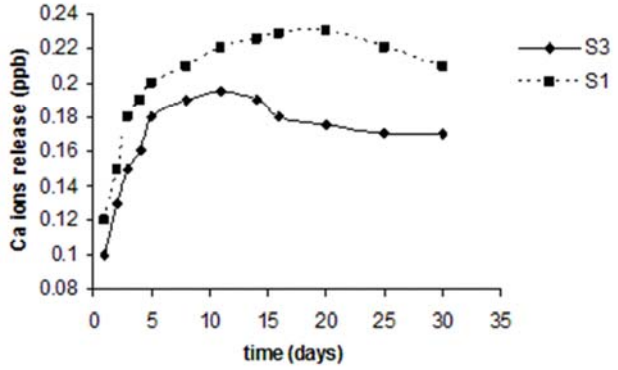

Fig. 7. The evolution in time of the release of Ca^{2+} and Ti ions

For sample S1, the dissolution process takes place after 7 days. It is suggested that the short term release of ions from dissolving calcium phosphate phases can be optimized. The results of this study indicate that the dissolution rate of coating at initial times of immersion is mainly attributed to the difference in the crystallinity of coating surface, and partly to the difference in porosity levels and amounts of recrystallized HA [38]. On the other hand, the release rate of calcium ions from the coating at longer times becomes dominant after the mineralization process.

Using ANOVA single factor analysis, in all the cases the probability $P<0.001$, we reject the null hypothesis. It implies that, for different periods of time, there are significant differences between the ions release values for titanium covered with HA and for the polished titanium, the values of ions release in the case of covered metal being smaller than ions release concentration for uncovered metal.

The Ti ions release in time permits an evaluation of corrosion rate (v_{corr}) according to the following expression:

$$v_{corr} = \frac{24 \times 365 \times \Delta m}{1000 \times \rho \times S \times t}, \text{[mm/y] [39]} \quad (1)$$

where: Δm - ion release [g]; ρ - titanium density [kg/m^3]; S - area [m^2], t-hours [h], 1000 - conversion factor for measurement units.

The corrosion rate calculated from ICP-MS determinations was compared with the rate from Tafel plots and is presented in Table 3. It may be observed a good correlation between corrosion rate obtained from potentiodynamical curves and corrosion rate from ions release analysis. The synergistic effect on stability of a nanostructure and of bioactive ceramic coating on Ti is found as well.

3.4. Cell adherence and viability

The bioperformance of implant materials is directly related to a strong cellular adhesion which, among other factors, is determined by the dimensions of surface topography.

Generally, the cells adhere to biomaterial surfaces initially by attaching to a preadsorbed protein network named extracellular matrix (ECM) or to neighbouring cells.

In accordance with literature data [28], the number of adhered cells on the smallest 30 nm diameter nanotubes was notably higher than for all the other sizes of nanotubes. This implies that cell behaviour is size dependent, having an optimum vitality for a specific dimension. As a quantified result in our experiments, MTT assay (Fig. 8) demonstrated that HGF-1 cells grown on nanotubes displayed a cell growth value of 101.4% viability higher than that of the cells grown on the native passive layer with 98.3% viability and than cell viability of TiO_2 obtained in electrolyte without fluoride which is 99.4%.

Such a difference is not significant, and confirms previous findings [28] regarding the behaviour of proteins on the higher diameter (100 nm) nanotubes which seem to adhere sparsely at the top wall surface, due to the presence of nanotube pore spaces. However, despite the fact that the relation between surface physical-chemical properties and cell behavior at the interface is not totally predictable [40-42], the cell viability values tend to increase in the same range as stability: Viability S3> Viability S2> Viability S1. This range corresponds to the more hydrophilic and stable structure in Hank environment, with less ion release, confirming that bioceramic coating on nanotubes structure leads to a synergetic effect in enhancing performance of an implant Ti material.

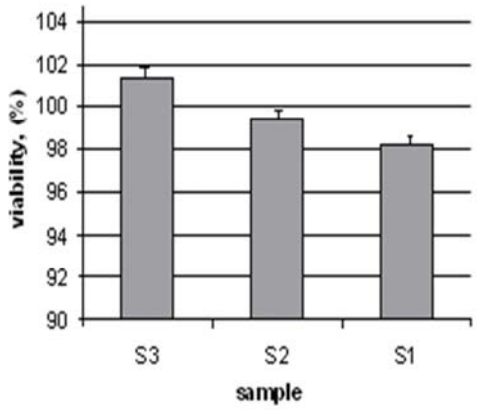

Fig. 8. Cell viability of the samples a) S1, b) S2, c) S3.

4. Conclusions:

1. We succeded to perform anodizing procedure in two different conditions and various TiO_2 structures from porous surface of a mixture of oxides to TiO_2 nanotubes with 60 nm diameters covered with biomimetic coatings.

2. From the point of view of corrosion, all studied samples had corrosion rates in Hank solution corresponding to classes of stability from stable to perfect stable. The architecture with nanotubes exhibited the higher stability in Hank solution after immersion in simulated body fluid, confirming the synergistic effect of hybrid structure (nanotubes + ceramic coating) on corrosion resistance of Ti implant.

3. ICP-MS determinations regarding the release of Ti ions sustain electrochemical results and corrosion rates obtained from ICP-MS determinations are close to the values obtained from Tafel plots.

4. The results of SEM and AFM microscopies and contact angle measurements permitted to establish correlation between surface features and sample stability. The nanotubes have contributed to the increase of surface roughness and surface area. After depositing the hydroxyapatite, the corresponding surfaces exhibited remarkably reduced contact angles and had better stability.

5. Biocompatibility evaluated from cell culture shows that the variation of cell viability represents a small enhancement of biocompatibility of coated nanotubes, and corresponds to contact angle decrease to more hydrophilic values. Having a smaller corrosion rate as well, this behavior sustains the idea that bioceramic coating on nanostructure leads to an enhance of performance

Acknowledgements

This work was supported by CNCSIS –UEFISCSU, project number PNII – IDEI 1712/2008.

R E F E R E N C E S

[1] *E.B. Taddei, V.A.R. Henriques, C.R.M. Silva, C.A.A. Cairo*, Mater. Sci. Eng., **vol. 24**, 2004, pp 683-687

[2]*M. Mindroiu , E. Cicek , F. Miculescu , I. Demetrescu ,* Rev. Chim. (Bucharest), **vol. 58 (9)**, 2007, pp. 898-903

[3] *A.K. Shukla, R. Balasubramanian*, Corros. Sci., **vol.** 48, 2006, pp 1696-1720

[4] *I.V. Branzoi, M. Iordoc, F. Branzoi,* U.P.B. Sci. Bull., **vol. 71**, 2009, pp 31-40

[5] *F. Variola, F. Vetrone, L. Richert, P. Jedrzejowski, J.H. Yi, S. Zalzal, S. Clair, A. Sarkissian, D.F. Perepichka, J.D. Wuest, F. Rosei, A. Nanci*, Small, **vol. 5 (9)**,2009, pp 996-1006

[6] *I. Demetrescu, D. Ionita, C. Pirvu, D. Portan*, Mol. Cryst. Liq. Cryst., **vol. 521**, 2010, pp 195-203

[7] *T. Hanava*, Mater. Sci. Eng., **vol. A 267**, 1999, pp 260-266

[8] *S. Popescu, I. Demetrescu, V.Mitran, A.Gleizes*, Mol. Cryst. Liq. Cryst., **vol. 483**, 2008, pp 266-274

[9] *M.V.Popa, I. Demetrescu, D. Iordachescu, A. Cîmpean, E.Vasilescu, P. Drob, C.Vasilescu, M. Istrătescu*, Mater. Corros., **vol. 58(9)**, 2007, pp 687-695
[10] *N.D. Tomashov*, Corros. Sci., **vol.1**, 1961, pp 77-111
[11] *G.T. Burstein, L.L. Shreir, R.A. Jarman* in Corrosion, Metal/Environment reactions, Third Ed. Butterworth-Heinemann, Great Britain, 1994, pp. XV, XXIII.
[12] *C. Yao, T.J. Webster*, J. Nanosci. Nanotechnol., **vol 6**, 2006, pp 2682-2692
[13] *I. Demetrescu, C. Pirvu, V. Mitran*, Bioelectrochemistry, **vol 79**, 2010, pp 122-129
[14] *C. Cao, J. Li, X. Wang, X. Song, Z. Sun*, J. Mater .Res. doi: 10457/jmr. 2010.33
[15] *T.S.B. Narasaraju, D.E. Phebe*, J. Mater. Sci., **vol.** 3, 1996, pp 1-21
[16] *A. Kodama, S. Bauer, A.Komatsu, H. Asoh, S. Ono, P. Schmuki*, Acta Biomater., **vol. 5**, 2009, pp 2322-2330
[17] *G. Ciobanu, G. Carja, O. Ciobanu, I. Sandu, A. Sandu*, Micron, **vol. 40**, 2009, pp 143-146
[18] *H.H. Park, S. Park, K.S. Kim, W.Y. Jeon, B.K. Park, H.S. Kim, T.S. Bae, M.H. Lee*, Electrochim. Acta, **vol. 55 (20)**, 2010, pp 6109-6114
[19] *B. Basar, A. Tezcaner, D. Keskin, Z. Evis*, Ceram. Int., **vol. 36 (5)**, 2010, pp 1633-1643
[20] *M Mîndroiu, C Pîrvu, Raluca Ion, I Demetrescu*, Electrochim. Acta, **vol. 56 (1)**, 2010, pp 193-202
[21] *D. Portan, D. Ionita, I. Demetrescu*, Key Eng. Mater., **vol. 415**, 2009, pp 9-12
[22] *Karla S. Brammer, Seunghan Oh, John O. Gallagher, Sungho Jin,* Nano Lett., **vol. 8 (3)**, 2008, pp 786-793
[23] *F. Barrere, C.M.van der Valk, R.A.J. Dalmeijer, G. Meijer, C.A. van Blitterswijk, K. de Groot, P. Layrolle*, J. Biomed. Mater. Res., Part A, **vol. 66**,2003, pp 779-788
[24] *F. Barrere, C.M. van der Valk, R.A.J. Dalmeijer, K. de Groot, P. Layrolle*, J.Biomed. Mater. Res., Part B, **vol. 67**, 2003, pp 655-665
[25] *E Aldea, N. Badea, I. Demetrescu*, Rev. Chim. (Bucharest), **vol. 58**, 2007, pp 918-922
[26] *E. Boanini, P. Torricelli, M. Gazzano*, Biomaterials, **vol. 27**, 2006, pp 4428-4433
[27] *J. Forsgren, F. Svahn*, Acta Biomater., **vol. 3**, 2007, pp 980-984
[28] *K. S. Brammer, O. Seunghan, C.J. Cobb, L.M. Bjursten, H. van der Heyde, S. Jin*, Acta Biomater. 2, **vol. 5 (8)**, 2009, pp 3215-3223
[29] *I. Demetrescu, D. Ionita, D. Iordachescu, A. Cimpean, D. Portan*, Proceedings of ICBFS, 2010, pp 156-160
[30] ASTM F 2129-01 Tests method for conducting cyclic potentiodynamic measurements to determine corrosion susceptibility of small implant devices. ASTM International West Conshococken PA 2003.
[31] *X. Zhang, X.L., H., Fan, X., Liu*, Bioceramics, **vol. 19**, 2007, pp 581-584
[32] *A. Stoch, W., Jastrzebski, A., Brozek, J., Stoch, J., Szaraniec, B., Trybalska, G., Kmita*, J Mol Struct., vol. 555, 2000, pp 375-382
[33] *J.M. Macak, H. Tsuchiya, P. Schmuki*, Angew. Chem. Int. Ed. Engl., **vol. 44**, 2005, pp 2100-2102
[34] *J.M. Macak, P. ,* Electrochim. Acta , **vol. 52**, 2006, pp 1258-1264
[35] *J. Park, S. Bauer, K.A. Schlegel, F.W. Neukam, K. von der Mark, P. Schmuki*, Small, **vol. 5**, 2009, pp 666-671
[36] ISO 8044/2000: Corrosion of metals and alloys. Basic terms and definitions 2000.
[37] *W.Q. Yu, J. Qiu, L. Xu, F.Q. Zhang*, Biomed. Mater., **vol. 4**, 2009, pp 065012- 065018
[38] *O. Grafmann, R. Heimann*, J. Biomed. Mater. Res., **vol. 53**, 2000, pp 685-693
[39] ASTM G 102 -89 (1999)" Standard Practice for Calculation of Corrosion Rates and Related Information from Electrochemical Measurements
[40] *A.S.G. Curtis, P. Clark*, Crit. Rev. Biocomp., **vol. 5**, 1990, pp 343-362
[41] *M. Bigerelle, K. Anselme*, Eur. Cell. Mater**., vol. 7**, 2004, pp 7
[42] *J. Vitte, A. M. Benoliel, A. Pierres and P. Bongrand*, Eur Cell Mater., **vol. 7**, 2004, pp 52-63